


# Effect of Peritumoral Bupivacaine on Primary and Distal Hyperalgesia in Cancer-Induced Bone Pain

This article was published in the following Dove Press journal:  
*Journal of Pain Research*

Sumi Elizabeth Mathew\*  
Pallavi Madhusudan\*  
Sahadev A Shankarappa 

Center for Nanosciences & Molecular  
Medicine, Amrita Institute of Medical  
Sciences and Research Center, Amrita  
Vishwa Vidyapeetham University, Kochi,  
Kerala 682041, India

\*These authors contributed equally to  
this work

**Background:** Cancer-induced bone pain (CIBP) is a debilitating chronic pain condition caused by injury to bone nerve terminals due to primary or metastasized bone tumors. Pain manifests as enhanced sensitivity, not only over the affected bone site but also at distal areas that share common nerve innervation with the tumor. In this study, we aim to understand how tumor-induced primary and distal pain sensitivities are affected by bupivacaine-induced block of bone nerve endings in a rat model of CIBP.

**Methods:** MRMT-1 breast cancer cells were injected into the proximal segment of tibia in female Sprague–Dawley rats. Radiograms and micro-CT images were obtained to confirm tumor growth. Bupivacaine was injected peritumorally at day 7 or day 14 post-tumor induction, and withdrawal thresholds in response to pressure and punctate mechanical stimulus were recorded from the knee and hind-paw, respectively. Immunohistochemical studies for the determination of ATF3 and GFAP expression in DRG and spinal cord sections were performed.

**Results:** Rats developed primary and distal hyperalgesia after MRMT-1 administration that was sustained for 2 weeks. Peritumoral administration of bupivacaine in 7-day post-tumor-induced (PTI) rats resulted in a reversal of both primary and distal hyperalgesia for 20–30 mins. However, bupivacaine failed to reverse distal hyperalgesia in 14 day-PTI rats. ATF3 and GFAP expression were much enhanced in 14 day-PTI animals, compared to 7 day-PTI group.

**Conclusion:** Results from this study strongly suggest that distal hyperalgesia of late-stage CIBP demonstrates differential characteristics consistent with neuropathic pain as compared to early stage, which appears more inflammatory in nature.

**Keywords:** bupivacaine, epidermal nerve fiber, primary hyperalgesia, distal hyperalgesia, cancer-induced bone pain

## Introduction

Cancer-induced bone pain (CIBP) is a debilitating complication arising due to the presence of a primary malignant tumor, or more commonly a metastasized mass within bony tissue. Incidentally, pain is the most common presenting symptom of bone cancer for over two-thirds of patients with advanced breast and prostate cancer showing metastasis to the bone.<sup>1,2</sup> CIBP is typically characterized as a dull background pain, with or without movement-evoked pain<sup>3</sup> precipitated most likely by intense excitation of bone nerve endings,<sup>4</sup> along with the excitatory firing of central neurons in the spinal cord.<sup>5</sup> The current management strategy to address CIBP is to remove the tumor (by radiation therapy or surgical resection), and/or use of systemic analgesic drugs.<sup>6</sup> Though the current line of pain management provides

Correspondence: Sahadev A Shankarappa  
Center for Nanosciences and Molecular  
Medicine, Amrita Institute of Medical  
Sciences and Research Center, Amrita  
Vishwa Vidyapeetham University, Kochi,  
Kerala 682041, India  
Tel +91 4842 801234 (Ext 8705)  
Email sahaddevs@icloud.com

adequate pain relief in the majority of patients with CIBP, about 20% still experience unsatisfactory pain control.<sup>7</sup> Hence, novel strategies and further understanding of the mechanisms behind CIBP are urgently required.

Bone peripheral nerve endings and their role in the development of CIBP is an area that has been less explored. About 70% of peripheral nerve endings of bone are located underneath the periosteum, while the remaining 30% are found in the cortical and trabecular regions.<sup>8</sup> The nerve fibers innervating the bone are mainly of sensory and sympathetic origin, contributing to bone vascularization, matrix differentiation, and osteocyte metabolism.<sup>4,9</sup> Previous studies have shown that lytic tumors in the bone sensitize the unmyelinated C fiber nociceptors and the thinly myelinated A fiber neurons in the dorsal horn of the spinal cord, resulting in persistent pain.<sup>10</sup> Interestingly, the mechanism of pain generation in CIBP has been attributed to both inflammatory and neuropathic components. Features of inflammatory pain have been linked to the release of factors such as bradykinin,<sup>11</sup> endothelins,<sup>12</sup> and Interleukin-6<sup>13</sup> by cancer stromal cells within the bone matrix, while the neuropathic component is mainly due to sensitization of neurons in the spinal cord, secondary to tumor-induced axonal injury.<sup>14</sup> In addition, dense sprouting of peripheral nerve fibers has also been noted in tumor-bearing bone.<sup>15</sup>

Aberrant excitation of the tumor-affected bone nerve fibers has been attributed to the development of increased pain sensitivity over the tumor site, called primary hyperalgesia. Curiously, distal hyperalgesia is also observed at body sites that are quite remote from the tumor, and is generally considered to arise due to central neural involvement.<sup>16,17</sup> Previous studies have demonstrated that blocking peripheral nerve signals proximal to a nerve lesion can modulate the sensitization of central neurons in the spinal cord.<sup>18</sup> Relatedly, in this study, we wanted to further understand the nature of primary and distal hyperalgesia in CIBP. We, therefore, used bupivacaine, a strong local anesthetic agent, to block peripheral nerve fiber function around the tumor, and determined its effect on primary and distal hyperalgesia as a function of time.

## Materials and Methods

### Animal Care

Adult, female Sprague–Dawley rats weighing 200–250 g were housed in pairs, allowed standard rat diet and water ad libitum, and maintained on 10h/14h light/dark cycle. The

study was conducted under protocols approved by the Institutional Animal Ethical Committee (IAEC) (IAEC/2016/1/4), Amrita Institute of Medical Sciences, Kochi, India, in accordance with guidelines set forth by the Committee for Control and Supervision of Experiments on Animals (CPSCSEA), Government of India.

### Animal Model of CIBP

Bone tumor was induced in rats by injecting syngeneic breast cancer cell line, MRMT-1 (Riken, Japan) into the proximal end of tibia. MRMT1 cells (passage no. 10–13), were cultured in vitro 5% CO<sub>2</sub> at 37°C, in medium containing RPMI 1640 (Lonza, USA), 10% heat-inactivated fetal bovine serum (FBS) (Invitrogen, USA) and 1% penicillin-streptomycin (Invitrogen, USA). Cells were trypsinized and centrifuged at 200 g (Eppendorf, Model 5810R, Germany) for 5 min and counted. The cells were re-suspended in HBSS (Lonza, USA) at a concentration of  $3 \times 10^7$  cells/mL, and maintained at 4°C for administration into animals the same day.

Animals were anesthetized using an intraperitoneal injection of ketamine-xylazine, followed by a ~5–8 mm incision on the left knee joint, just enough to allow the penetration of a 24-gauge needle into the proximal end of the tibia. Ten  $\mu$ L of MRMT-1 cell suspension containing  $3 \times 10^5$  cells were injected slowly using a 50  $\mu$ L Hamilton syringe, into the anterolateral part of the proximal tibia, just after penetrating the articular cartilage. The incision was closed using tissue adhesive, and the animal was allowed to recuperate. Animals in the sham group received heat-killed MRMT-1 cells (cells exposed to 100°C for 30–45 min) and were exposed to all other conditions similar to the experimental group.

### Imaging Studies

Hind-limbs of anesthetized animals were radiographically imaged (GE OEC 9600 C-Arm, USA) on 7- and 14-day post-tumor induction (PTI), and the obtained radiograms were analyzed by a blinded observer. Animals were sacrificed and hind limbs collected for histology, and micro-CT imaging. Tibiae were scanned using microcomputed tomography (MILabs, Netherlands) with 8.8 voxel size, and 3D reconstructions were carried out with a dedicated visualization software (MILabs, Netherlands).

### Sensory and Motor Behavioral Tests

Tactile, thermal, and pressure responsiveness were measured separately on all animals, every 2 days, till the end of the study period. Enhanced pressure responsiveness over the knee joint (site of tumor induction) was measured as an

indicator of primary hyperalgesia. Pressure responsiveness was measured by applying graded mechanical pressure using a pressure application meter (PAM, Ugo Basile, Italy). A pressure-sensitive probe was gradually pressed against the tumor mass, until the animal reflexively removed the limb, and the force required to elicit the withdrawal response was recorded. Recordings were repeated thrice per animal, with a 5-min interval between each recording, and the mean value considered as the withdrawal threshold.

Tactile responsiveness elicited from the hind paw (distal from tumor site) was used to determine distal hyperalgesia. Measurement of tactile responsiveness has been described elsewhere,<sup>19</sup> but briefly, measurements were performed using calibrated Semmes Weinstein monofilaments (IITC Life Sciences, USA), and quantified by the Up-Down method of Dixon.<sup>20</sup> Animals were acclimatized to a wire-mesh bottom, followed by probing of the hind-paw with the monofilaments for at least 8 s, with sufficient force that caused slight buckling of the filaments. A reflexive withdrawal of the limb away from the testing probe was considered as a positive response. Testing began with a 2 g mass-force monofilament, followed by a “higher” or “lower” grade filament depending on the previous paw response. The mass-force required to elicit a 50% withdrawal response rate was calculated as previously described.<sup>19</sup> Each recording was repeated thrice per animal and the mean value considered as the paw-withdrawal threshold.

Thermal responsiveness was quantified using a microprocessor-controlled hot plate (IITC Life Sciences, USA). The hind paw of acclimatized animals was gently placed on the surface of the hot plate heated to 56°C. The time taken by the animal to reflexively remove its limb from the heated surface was recorded. Each limb was alternated three times, and the mean value considered as the withdrawal latency.

To test motor strength, rats were held over a digital weighing balance, in a manner where the animal was allowed to bear weight on one hind paw at a time.<sup>21</sup> The maximum weight borne by the animal was recorded. Each recording was repeated three times, and the mean value considered as the extensor postural thrust.

## Peritumoral Injection of Bupivacaine

Bupivacaine hydrochloride solution (0.5% w/v) was prepared in 0.9% saline and filter-sterilized (0.22 µm syringe filter). Bupivacaine was injected in sham and tumor-induced rats, immediately after a short inhalational exposure to 2% isoflurane. A 24-gauge needle was used to inject 150 µL of bupivacaine solution at the base of the tumor as it arises from

the bone. The injection site was digitally palpated during the course of needle insertion to ensure that the needle tip does not enter the tumor mass. Care was taken to inject the local anesthetic primarily into the bone around the tumor, without any infiltration into the tumor mass. All animals received bupivacaine injection on days 7 and 14 PTI, with each animal being tested for pain withdrawal threshold.

## Immunohistochemistry

Immunohistochemical analysis was performed on dorsal root ganglion (DRG) and spinal cord sections harvested from day 7 and day 14 PTI rats to determine the expression levels of ATF3 and GFAP, respectively. Animals were perfused with 4% (w/v) paraformaldehyde in 0.1 M PBS and post-fixed in 4% (w/v) paraformaldehyde overnight. Following tissue fixation and dehydration, DRG's and spinal cord tissue sections were embedded in paraffin blocks and 5 µm thin sections were cut using a microtome. DRG sections were stained with monoclonal mouse anti-ATF3 (1:500) antibody (Abcam, USA), and counterstained with DyLight 488 (10 µg/mL) (Vector Labs, USA) while, spinal cord sections were stained with polyclonal rabbit anti-GFAP (1:100) antibody (Abcam, USA), and counterstained using DyLight 549 (10 µg/mL) (Vector Labs, USA). DRG sections harvested from day 7 and day 14 CIBP animals (lumbar levels L4 to L5) with 4 sections per animal were examined using a Leica 3000B fluorescent microscope. ATF3 positive cells were calculated by counting the total number of cells and the number of ATF3 positive cells per field. For GFAP expression, spinal cord sections harvested from day 7 and day 14 CIBP animals with three sections per animal (consisting of four non-overlapping images per section) were utilized to measure the GFAP positive area per field using ImageJ (NIH) software, as described elsewhere.<sup>18</sup>

## Statistics

All data are represented as mean ± standard deviation (SD). Difference in mean values among experimental and control groups was tested using one-way, or two-way ANOVA, using GraphPad Prism version 7.0 for Mac (GraphPad Software, La Jolla California USA).

## Results

### Osteolytic Lesions in the CIBP Model of Rat

Female SD rats were injected with the syngeneic MRMT-1 breast cancer cells into the proximal end of left tibia, while the contralateral limb was used as control. Cells were

implanted just below the epiphyseal cartilage after penetration through the articular cartilage. On gross examination, a smooth swelling and palpable mass were noted (c.a 2–3 mm) at the site of tumor cell injection after 4–5 days, which increased in size over the period of study. On palpation, the mass was found to be fixed to the underlying tibial head, and the lower borders could not be differentiated from the bone. Radiographs of the knee joint obtained from day 14 PTI rats showed distinct osteolytic lesions that appeared translucent and ill-defined, covering the proximal one-third of tibia (Figure 1A). Micro-CT images of the tumor-bearing bone further confirmed the presence of large lytic lesions that had eroded the surface of the proximal end of tibia (Figure 1C and D). Smaller lytic lesions were also observed in the distal end of the femur (Figure 1D), most likely due to the extravasation of the tumor cells into the knee joint. Despite the aggressive nature of the induced tumor, rats appeared active, with no loss in body weight (Figure 1B) or change in gait for the entire 14-day period of the study.

## Primary and Distal Hyperalgesia in CIBP

To assess the development of primary and distal hyperalgesia in tumor injected animals, evoked limb-withdrawal behavior was tested by application of appropriate stimuli around the knee and hind paw, respectively. Behavioral response to the application of mechanical pressure over the local tumor site was used as a measure of primary pressure hyperalgesia,<sup>22</sup> while the response to the application of tactile stimulus at the hind paw was used as a measure of distal punctate hyperalgesia.<sup>23</sup>

Animals demonstrated enhanced responsiveness to the application of milder pressure at the tumor site, compared to the non-tumor bearing contralateral control knee ( $P < 0.05$ ,  $n = 4$ , Figure 2A). This form of primary pressure hyperalgesia in the ipsilateral limb was observed starting on day 3 and was maintained throughout the duration of the study. Similarly, animals showed increased sensitivity towards tactile probing of the hind paw in the tumor-afflicted limb compared to the contralateral limb ( $P < 0.05$ ,  $n = 10$ , Figure 2B), suggestive of distal hyperalgesia. The onset of distal hyperalgesia was also observed around day 3, and remained throughout the duration of the study. In stark contrast, animals demonstrated no difference in the hind paw responsiveness to thermal stimulus in both tumor-afflicted and non-afflicted limbs ( $P < 0.05$ ,  $n = 10$ , Figure 2C). Our findings agree well with previous studies that have showed a normal response to thermal stimulus in remote hyperalgesia.<sup>24,25</sup> In addition, rats injected with heat-

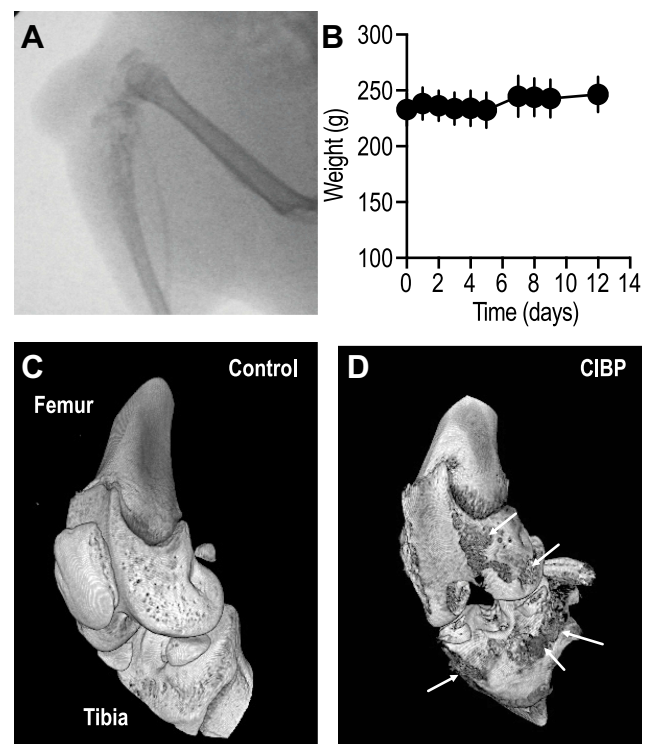


**Figure 1** Rats injected with MRMT1 breast cancer cells demonstrated osteolytic lesions on (A) radiographs, and lytic lesions on gross examination. (B) The gross body weight of the tumor-bearing animals throughout the experimental duration remained constant. Data shown are mean  $\pm$  S.D., obtained from 18 rats. (C–D) Micro-CT images showed clear degradation of the periosteal layer along with degradation of the underlying bone tissue (arrows).

inactivated MRMT-1 cells in the proximal tibia did not show any change in response to pressure or punctate stimulus (Supplementary Figure 1A and B).

Since motor pathways partly determine the interpretation of sensory behavioral tests, we measured the thrust exerted by the extensor muscles of the hind limb (extensor postural thrust) as an indicator of limb motor strength. Both, ipsilateral and contralateral limb exerted similar force ( $P > 0.05$ ,  $n = 10$ , Figure 2D), suggesting that the motor component was unaffected by tumor growth in the proximal tibia.

## Sensitivity of Primary and Distal Hyperalgesia to Local Bupivacaine in CIBP

To determine the effect of bone-nerve fiber blockade on primary and distal hyperalgesia, bupivacaine was injected in a manner where the drug solution was administered deep near the base of the tumor as it projects from the bone. Care was taken not to inject the drug into the tumor tissue, but the needle was advanced far enough to enter the articulating cartilage and the bone. Vehicle treated tumor-

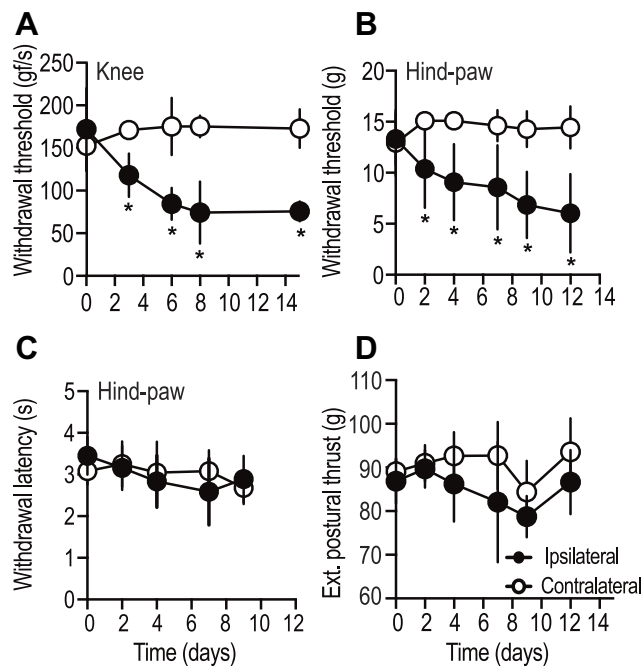


**Figure 2** Tumor-afflicted limbs of rats injected with MRMT1 breast cancer cells demonstrated hyperalgesia at both primary tumor site (knee) and a distal site (hind paw). (A) Local pressure evoked withdrawal response, (B, C) mechanical-stimulus evoked and thermal-stimuli evoked withdrawal response (hind paw), and (D) extensor postural thrust (hind paw) was recorded up to 10–14 days post-tumor induction. Data shown are mean  $\pm$  S.D., obtained from  $n = 4$  rats (A), and  $n = 10$  (B, C, D). \*indicates  $P$  value of  $<0.05$ , two-way ANOVA along with correction for multiple comparisons using the Bonferroni method.

bearing rats were used as controls ([Supplementary Figure 2A](#) and [B](#)). Animals were injected with bupivacaine on days 7 and 14 PTI. These time points were chosen to represent short-term and long-term consequences of CIBP, respectively. Tumor-bearing rats injected with bupivacaine showed pressure-induced withdrawal thresholds that were significantly higher ( $P < 0.05$ ,  $159.8 \pm 29.1$  gf/s,  $n = 4$ , [Figure 3A](#) and [C](#)), compared to baseline measurements (time = 0 min,  $78.3 \pm 13.6$  gf/s). The observed bupivacaine-induced blockade of primary pressure hyperalgesia at the tumor site was maintained for a period of 20–30 mins, in both day-7 and -14 PTI groups. Similarly, responsiveness to the punctate stimulus of the hind paw, after bupivacaine injection in the day-7 PTI rats demonstrated withdrawal thresholds that were significantly higher ( $P < 0.05$ ,  $11.9 \pm 4.09$  g,  $n = 16$ , [Figure 3B](#)) compared to baseline recordings. The effect of bupivacaine was observed for a duration of 4 hrs, after which the withdrawal threshold returned to baseline ([Figure 3B](#)). In stark contrast, bupivacaine did not induce any change in the withdrawal thresholds obtained from day-14 PTI rats ( $P > 0.05$ ,  $10.02 \pm 5.24$  g,  $n = 10$ , [Figure 3D](#)). These findings strongly suggest that CIBP-induced late distal punctate

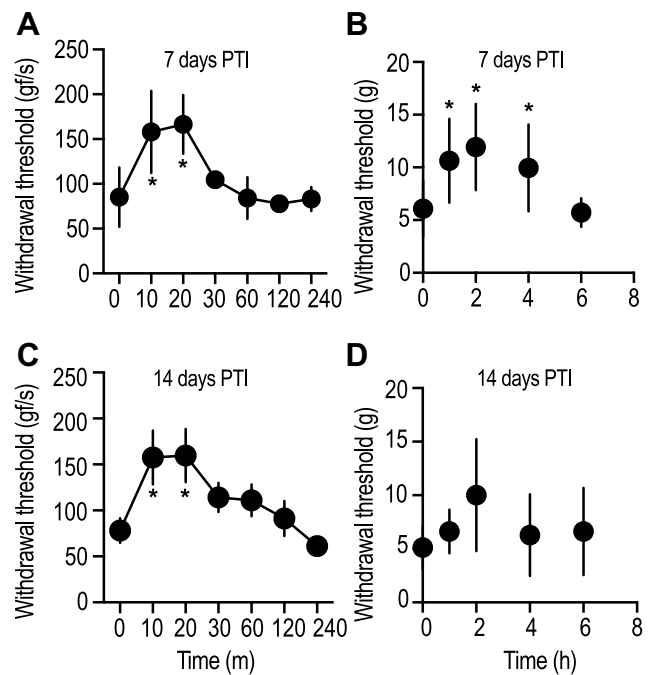


**Figure 3** Peritumoral injection of bupivacaine solution reversed tumor-induced primary-pressure-evoked hyperalgesia for up to 20 mins in both, early and late stage of CIBP. Meanwhile, tumor-induced distal hyperalgesia was abolished up to 4 hrs at the early stage (7 days post-tumor induction), but not in the late stage (14 days post-induction) of CIBP condition. Data shown are mean  $\pm$  S.D., from four rats (A, C), and 16 rats (B, D). \*indicates  $P$  value of  $<0.05$ , one-way ANOVA, with Dunnett's multiple comparison test. (Data points indicate ipsilateral limb).

hyperalgesia does not respond to peripheral blockade of bone nerve terminals.

## Expression of ATF3 and GFAP in the DRG and Dorsal Horn Cells of CIBP Animals

Since distal punctate hyperalgesia in rats with long-standing bone tumors was not affected by peritumoral bupivacaine, we wanted to determine the expression of injury markers in neurons that innervate the area where distal hyperalgesia was elicited. It is interesting to note that the nerve innervation to the skin site overlying the proximal tibia is via fibers arising in the L1-3 spinal cord lamina,<sup>26</sup> while the skin from the hind paw receives innervation from the L4-5 lamina.<sup>27</sup> DRG sections harvested from L4-5 regions were stained for the injury marker, activating transcription factor 3 (ATF3) ([Figure 4A–E](#)). About 8–9% of DRG neurons from day-7 CIBP animals demonstrated ATF3 positivity, which increased to 20% by day 14 ([Figure 4E](#)). Only those DRG neurons that showed brightly stained nucleus were counted as ATF3 positive cells ([Figure 4C](#), inset). DRG sections harvested

from the contralateral side showed minimal to no ATF3 positivity.

Similarly, L4-5 spinal cord sections were stained for Glial fibrillary acidic protein (GFAP) (Figure 4F–J), as a marker for astrocyte activation, and a sign of central sensitization. The dorsal horn region of the spinal cord sections demonstrated marked GFAP staining that was distinctly increased in day 14 animals as compared to day 7, though there was no statistical difference between the two groups ( $P > 0.05$ ,  $n = 4$ ). Dorsal horn sections from the contralateral side showed minimal GFAP staining, except for two animals which showed strong contralateral GFAP staining 14 days after tumor induction (Figure 4J). Detection of GFAP positive cells on the contralateral side of nerve injury is not uncommon, and has been reported by other studies as well,<sup>18,28</sup> possibly due to the spread of injury-induced aberrant electrogenic signals to the opposite segment.<sup>29</sup> Overall, these findings indicate that a central neuronal injury due to tumor-induced peripheral nerve damage is observed 7 days after tumor induction, which progresses and becomes more robust by day 14.

## Discussion

A large population of patients with metastasized tumors to the bone not only experience hyperalgesia directly over the tumor site<sup>30</sup> but also to distal sites.<sup>31</sup> Primary hyperalgesia arising directly from the site of tumor has been attributed to the pathological reorganization of the peripheral nerve terminals located within the bone–tumor interface,<sup>32</sup> aberrant sprouting of nerve fibers,<sup>15</sup> tumor-induced compression of axons,<sup>33</sup> and exposure of bone-peripheral nerve terminals to various nociceptive factors within the tumor microenvironment.<sup>34</sup> By contrast, the onset of distal hyperalgesia is attributed to cellular changes that occur in the central nervous system, collectively termed as central sensitization. It is interesting to note that the term “secondary hyperalgesia” has been used in overlapping context with distal hyperalgesia, to describe pain sensitivity in remote areas,<sup>22,35</sup> as well as in the immediate vicinity of an injury.<sup>16,17</sup> Since in this study, we are addressing hyperalgesia in an area much further away from the primary tumor site, we chose to use “distal hyperalgesia” to maintain distinction.

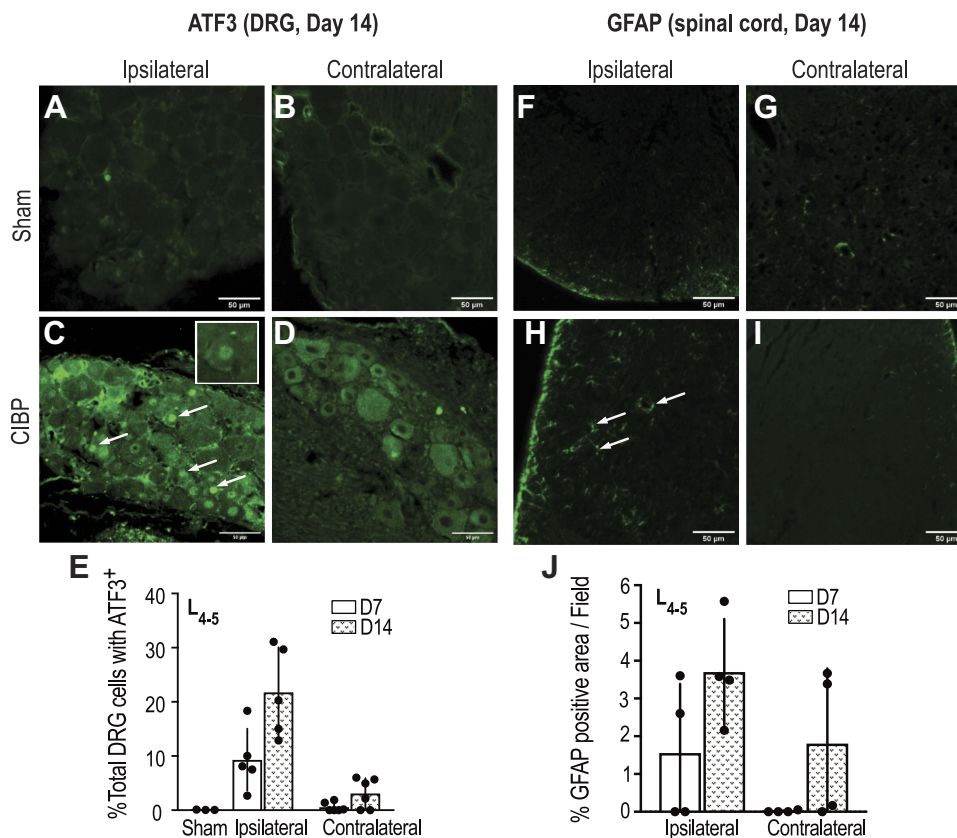


**Figure 4** Representative images of ATF3 positive cells (arrows) in lumbar (L<sub>4-5</sub>) DRG sections obtained at day 14 from the ipsilateral or contralateral side of the sham (A, B) and tumor-bearing animals (C, D). Histogram showing ATF3 staining quantification in (E). Similarly, representative images of the spinal cord section from the lumbar area stained for GFAP positive cells (arrows) from sham (F, G) and tumor-bearing animals (H, I) and quantified in (J) ( $n=4$ ).

## Early and Late Hyperalgesia

In this study, we have attempted to understand the bupivacaine sensitivity of bone-nerve terminals and its ensuing effect on primary and distal hyperalgesia at various time points during the course of CIBP. We observed that female rats developed primary pressure hyperalgesia, and distal punctate hyperalgesia, 2–3 days after tumor induction, and the initial onset of hyperalgesia preceded the occurrence of palpable tumor mass by 4–5 days. Previous studies have clearly shown that macrophages, T cells,<sup>36</sup> and neutrophils are actively recruited in and around the bone tumor,<sup>37</sup> resulting in an inflammatory response.<sup>38</sup>

Secretions from these inflammatory cells, including prostaglandins,<sup>39</sup> endothelin<sup>12</sup> and various other cytokines are primarily responsible for the activation of nociceptive receptors located on afferent bone fibers. Considering the short timeline for the development of pain hypersensitivity, this “early hyperalgesia” observed both at the knee and distally at the hind paw could primarily be due to an inflammatory response towards the injected cancer cells.

By the end of 2 weeks, both primary pressure hyperalgesia, and distal punctate hyperalgesia had increased in sensitivity to a point where the difference between early and late hyperalgesia (hyperalgesia at 2 weeks) was considerably large. This observation suggests that as early hyperalgesia progresses to late hyperalgesia, there may be changes, either at the bone sensory afferents, and/or centrally at the spinal cord that is responsible for the observed sustenance and increase in pain sensitivity. In this connection, it has been shown that spinal cord segments innervated by primary afferent neurons from tumor-bearing limbs undergo extensive neurochemical rearrangement.<sup>38</sup> Such central changes include astrocyte hypertrophy, increased extracellular glutamate, and enhanced expression of injury markers like ATF3, galanin, and c-Fos.<sup>40</sup> In addition, animals with CIBP have also been reported to demonstrate a shift in nociceptive to wide-dynamic range neuron ratio, which is thought to increase neuronal response-probability to low-threshold inputs, forming the basis for pain behavior.<sup>41</sup>

Even though our CIBP rats demonstrated punctate hyperalgesia, their response to thermal stimuli was similar to controls. This is consistent with previous studies that report the selective diminution of somatic sensitivity to tactile, but not to thermal stimuli, which has been attributed to the loss of epidermal innervation<sup>42</sup> or action of the endogenous opioid system.<sup>25</sup> However, it must be noted that there are other studies that have clearly observed marked hyperalgesia in response to

thermal stimulus in nerve-injured rats.<sup>41</sup> Reasons for differences in heat-induced pain behavior among different studies are still unclear but could be attributed to differences in the animal model, ambient temperature while testing, or the testing apparatus used.

## Bupivacaine Sensitivity

CIBP-induced primary pressure hyperalgesia was completely blocked by peritumoral bupivacaine at all-time points in the study. This was expected, primarily because bupivacaine, a known local anesthetic, blocks voltage-sensitive sodium channels in the peripheral axons and inhibits the generation of afferent signals.<sup>43</sup> In contrast, the effect of bupivacaine on CIBP-induced distal punctate hyperalgesia was quite different; early distal hyperalgesia was reversed by bupivacaine, while late distal hyperalgesia was not. This is interesting because it highlights the difference in the underlying cellular mechanism that is involved in the manifestation of early and late distal hyperalgesia. Early distal hyperalgesia appears to be associated with alteration in the sensitivity of distal peripheral neurons secondary to changes within the bone-nerve terminals, and not due to changes in the central nervous system. This was supported by the absence of ATF3 and GFAP expression in the lumbar DRG and spinal cord lamina of day 7 PTI rats, respectively (data not shown). However, late distal hyperalgesia appears to be more associated with central neuronal changes consistent with neuropathic mechanisms, as observed by the increase in ATF3 and GFAP expression in DRG and spinal cord lamina of day 14 PTI rats. This may also explain the non-responsiveness of late distal hyperalgesia to the peritumoral injection of bupivacaine. Here, it is important to add that ATF3, a member of the activating transcription factor/cAMP-responsive element binding protein (ATF/CREB) family of transcription factors, is known to be overexpressed in neurons under cellular stress.<sup>44</sup> Similarly, GFAP, a glial intermediate filament protein shows increased expression in activated astrocytes, and is commonly used as a marker of central sensitization in neuropathic pain conditions.<sup>45</sup>

One of the limitations of the study was that the tumor, in addition to eroding the bone, also extended into the joint and the surrounding soft tissue. Though such gross invasion of bone and its surrounding tissue are seen in clinical cases of metastasis,<sup>46</sup> experimentally it would involve the peripheral nerve fibers in the synovium as well. The majority of the synovial nerve fibers have been reported to be of sympathetic origin;<sup>47</sup> hence, the primary pressure hyperalgesia observed in this study could be partly mediated by these fibers. Alternatively, previous studies addressing CIBP have utilized

animal models where cancer cells are injected into a pre-drilled opening in the bone and sealed.<sup>41</sup> These models restrict the tumor within the bone, but also prevents local drug delivery to the vicinity of the tumor. In the current study, the tumor affects the superior end of the tibia, disrupting the integrity of the bone and cartilage, and protrudes out of the bone. This provides an avenue for administering bupivacaine peritumorally, and into the bone, for blocking bone-nerve terminals. With the development of novel delivery systems,<sup>48,49</sup> applications such as the above, hold much promise in managing acute and chronic phases of CIBP.

In conclusion, we have observed that late CIBP-induced-pain sensitivity in areas distal to the tumor site differs from that in the primary site in response to nerve terminal blockade in the tumor-afflicted bone. This could be due to the gradual progression of changes from an inflammatory origin, to a more neuro-pathic mechanism in the connected neurons. However, additional studies are required to better understand the role of bone-nerve terminals and their chronic involvement with a growing tumor that results in enhanced distal pain conditions.

## Data Accessibility

The data that support the findings of this study are available from the corresponding author upon reasonable request.

## Acknowledgments

We thank Dr. Shivaneesh Shah for her editorial support. We thank Dr. Siddaramaiah Gowda for technical assistance with micro CT imaging. We also thank Mr. Sunil and Mr. Sajith for technical assistance with radiography at the AIMS Central Animal facility.

## Author Contributions

SEM performed experiments, PM performed experiments and analyzed data, SS conceived the idea, analyzed data and wrote the manuscript. All authors contributed to data analysis, drafting or revising the article, gave final approval of the version to be published, and agree to be accountable for all aspects of the work.

## Funding

M. Tech Nanomedical project grant (DST, Govt. of India) to SEM, CSIR fellowship (DST, Govt. of India) to PM, and grants 6242-P75/RGCB/PMD/DBT/SDSA/2015, BT/PR24515/MED/30/1926/2017 (DBT, Govt. of India), and the Ramalingaswami fellowship (DBT, Govt. of India) to SS.

## Disclosure

SS reports grants from the Department of Science and Technology, Government of India and from the Department of Biotechnology, Government of India, during the conduct of the study. The authors declare no other possible conflicts of interest.

## References

- Wong SK, Mohamad NV, Giaze TR, Chin KY, Mohamed N, Ima-Nirwana S. Prostate cancer and bone metastases: the underlying mechanisms. *Int J Mol Sci*. 2019;20(10):2587. doi:10.3390/ijms20102587
- Pulido C, Vendrell I, Ferreira AR, et al. Bone metastasis risk factors in breast cancer. *ecancer*. 2017;11:1–17. doi:10.3332/ecancer.2017.715
- Honore P, Luger NM, Sabino MAC, et al. Osteoprotegerin blocks bone cancer-induced skeletal destruction, skeletal pain and pain-related neurochemical reorganization of the spinal cord. *Nat Med*. 2000;6(5):521–528. doi:10.1038/74999
- Mach DB, Rogers SD, Sabino MC, et al. Origins of skeletal pain: sensory and sympathetic innervation of the mouse femur. *Neuroscience*. 2002;113(1):155–166. doi:10.1016/S0306-4522(02)00165-3
- Dubin AE, Patapoutian A. Nociceptors: the sensors of the pain pathway. *J Clin Invest*. 2010;120(11):3760–3772. doi:10.1172/JCI42843.3760
- Chow E, van der Linden YM, Roos D, et al. Single versus multiple fractions of repeat radiation for painful bone metastases: a randomised, controlled, non-inferiority trial. *Lancet Oncol*. 2014;15(2):164–171. doi:10.1016/S1470-2045(13)70556-4
- Nersesyan H, Slavin KV. Current approach to cancer pain management: availability and implications of different treatment options. *Ther Clin Risk Manag*. 2007;3(3):381–400.
- Castañeda-coral G, Jimenez-andrade JM, Bloom AP, et al. The majority of myelinated and unmyelinated sensory nerve fibers that innervate bone express the tropomyosin receptor kinase A. *Neuroscience*. 2011;520:196–207. doi:10.1016/j.neuroscience.2011.01.039
- Jimenez-Andrade JM, Mantyh PW. Sensory and sympathetic nerve fibers undergo sprouting and neuroma formation in the painful arthritic joint of geriatric mice. *Arthritis Res Ther*. 2012;14(3):R101. doi:10.1186/ar3826
- Mantyh PW. Bone cancer pain: from mechanism to therapy. *Curr Opin Support Palliat Care*. 2014;8(2):83–90. doi:10.1097/SPC.000000000000048
- Sevcik MA, Ghilardi JR, Halvorson KG, Lindsay TH, Kubota K, Mantyh PW. Analgesic efficacy of bradykinin B1 antagonists in a murine bone cancer pain model. *J Pain*. 2005;6(11):771–775. doi:10.1016/j.jpain.2005.06.010
- Peters CM, Lindsay TH, Pomonis JD, et al. Endothelin and the tumorigenic component of bone cancer pain. *Neuroscience*. 2004;126(4):1043–1052. doi:10.1016/j.neuroscience.2004.04.027
- Ara T, DeClerck YA. Interleukin-6 in bone metastasis and cancer progression. *Eur J Cancer*. 2010;46(7):1223–1231. doi:10.1016/j.ejca.2010.02.026
- Falk S, Dickenson AH. Pain and nociception: mechanisms of cancer-induced bone pain. *J Clin Oncol*. 2014;32(16):1647–1654. doi:10.1200/JCO.2013.51.7219
- Mantyh WG, Jimenez-andrade JM, Stake JJ, et al. Blockade of nerve sprouting and neuroma formation markedly attenuates the development of late stage cancer pain. *Neuroscience*. 2010;171(2):588–598. doi:10.1016/j.neuroscience.2010.08.056. Blockade
- Hardy JD, Wolff HG, Goodell H. Experimental evidence on the nature of cutaneous hyperalgesia. *J Clin Invest*. 1950;115(1):115–140. doi:10.1093/oxfordjournals.bmb.a071408



17. Treede RD, Magerl W. Multiple mechanisms of secondary hyperalgesia. *Prog Brain Res.* 2000;129:331–341. doi:10.1016/S0079-6123(00)29025-0
18. Shankarappa S, Tsui JH, Kim KN, et al. Prolonged nerve blockade delays the onset of neuropathic pain. *Proc Natl Acad Sci U S A.* 2012;109(43):17555–17560. doi:10.1073/pnas.1214634109
19. Shankarappa SA, Piedras-Renteria ES, Stubbs EB Jr. Forced-exercise delays neuropathic pain in experimental diabetes: effects on voltage-activated calcium channels. *J Neurochem.* 2011;118(2):224–236. doi:10.1111/j.1471-4159.2011.07302.x
20. Chaplan SR, Bach FW, Pogrel JW, Chung JM, Yaksh TL. Quantitative assessment of tactile allodynia in the rat paw. *J Neurosci Methods.* 1994;53(1):55–63. doi:10.1016/0165-0270(94)90144-9
21. McAlvin BJ, Reznor G, Shankarappa SA, Stefanescu CF, Kohane DS. Local toxicity from local anesthetic polymeric microparticles. *Anesth Analg.* 2013;116(4):794–803. doi:10.1213/ANE.0b013e31828174a7
22. Sandkühler J. Models and mechanisms of hyperalgesia and allodynia. *Physiol Rev.* 2009;89(2):707–758. doi:10.1152/physrev.00025.2008
23. Barton NJ, Strickland IT, Bond SM, et al. Pressure application measurement (PAM): a novel behavioural technique for measuring hypersensitivity in a rat model of joint pain. *J Neurosci Methods.* 2007;163(1):67–75. doi:10.1016/j.jneumeth.2007.02.012
24. Cain DM, Wacnik PW, Simone DA. Animal models of cancer pain may reveal novel approaches to palliative care. *Pain.* 2001;91(1–2):1–4. doi:10.1016/S0304-3959(01)00287-1
25. Menéndez L, Lastra A, Fresno MF, et al. Initial thermal heat hypoalgesia and delayed hyperalgesia in a murine model of bone cancer pain. *Brain Res.* 2003;969(1–2):102–109. doi:10.1016/S0006-8993(03)02284-4
26. Williams SE, Black AC. Intrapartum lesions to the lumbar portion of the lumbosacral plexus: an anatomical review. *Eur J Anat.* 2019;23(2):83–90.
27. Points A. Neuroanatomy of acu-reflex points. *Acupunct Sport Trauma Rehabil.* 2011;88–131. doi:10.1016/b978-1-4377-0927-8.00008-7
28. Garrison CJI, Dougherty PM, Carlton SM, Carlton SM. Staining of glial fibrillary acidic protein (GFAP) in lumbar spinal cord increases following a sciatic nerve constriction injury. *Brain Res.* 1991;565(1):1–7. doi:10.1016/0006-8993(91)91729-k
29. Reisert I, Wildemann G, Grab D, Pilgrim C. The glial reaction in the course of axon regeneration: a stereological study of the rat hypoglossal nucleus. *J Comp Neurol.* 1984;229(1):121–128. doi:10.1002/cne.902290109
30. Svendsen KB, Andersen S, Arnason S, et al. Breakthrough pain in malignant and non-malignant diseases: a review of prevalence, characteristics and mechanisms. *Eur J Pain.* 2005;9(2):195–206. doi:10.1016/j.ejpain.2004.06.001
31. Caraceni A, Portenoy RK. An international survey of cancer pain characteristics and syndromes. *Pain.* 1999;82(3):263–274. doi:10.1016/s0304-3959(99)00073-1
32. Wacnik PW, Eikmeier LJ, Ruggles TR, et al. Functional interactions between tumor and peripheral nerve: morphology, algogen identification, and behavioral characterization of a new murine model of cancer pain. *J Neurosci.* 2001;21(23):9355–9366. doi:10.1523/jneurosci.21-23-09355.2001
33. Tsuzuki S, Park SH, Eber MR, Peters CM, Shiozawa Y. Skeletal complications in cancer patients with bone metastases. *Int J Urol.* 2016;23(10):825–832. doi:10.1111/iju.13170
34. Schmidt BL, Hamamoto DT, Simone DA, Wilcox GL. Mechanisms of Cancer pain. *Mol Interv.* 2010;10(3):164–178. doi:10.1124/mi.10.3.7
35. Jochmann E, Boettger MK, Anand P, Schaible HG. Antigen-induced arthritis in rats is associated with increased growth-associated protein 43-positive intraepidermal nerve fibres remote from the joint. *Arthritis Res Ther.* 2015;17(1):1–15. doi:10.1186/s13075-015-0818-8
36. Wang Z, Li B, Ren Y, Ye Z. T-cell-based immunotherapy for osteosarcoma: challenges and opportunities. *Front Immunol.* 2016;7(353):1–13. doi:10.3389/fimmu.2016.00353
37. Uribe-Querol E, Rosales C. Neutrophils in cancer: two sides of the same coin. *J Immunol Res.* 2015;2015:1–21. doi:10.1155/2015/983698
38. Mantyh PW, Clohisy DR, Koltzenburg M, Hunt SP. Molecular mechanisms of cancer pain. *Nat Rev Cancer.* 2002;2(3):201–209. doi:10.1038/nrc747
39. Vasko MR. Prostaglandin-induced neuropeptide release from spinal cord. *Prog Brain Res.* 1995;104(C):367–380. doi:10.1016/S0079-6123(08)61801-4
40. Peters CM, Ghilardi JR, Keyser CP, et al. Tumor-induced injury of primary afferent sensory nerve fibers in bone cancer pain. *Exp Neurol.* 2005;193(1):85–100. doi:10.1016/j.expneurol.2004.11.028
41. Urch CE, Donovan-Rodriguez T, Dickenson AH. Alterations in dorsal horn neurones in a rat model of cancer-induced bone pain. *Pain.* 2003;106(3):347–356. doi:10.1016/j.pain.2003.08.002
42. Beiswenger KK, Calcutt NA, Mizisin AP. Dissociation of thermal hypoalgesia and epidermal denervation in streptozotocin-diabetic mice. *Neurosci Lett.* 2008;442(3):267–272. doi:10.1016/j.neulet.2008.06.079
43. Epstein-Barash H, Shichor I, Kwon AH, et al. Prolonged duration local anesthesia with minimal toxicity. *Proc Natl Acad Sci U S A.* 2009;106(17):7125–7130. doi:10.1073/pnas.0900598106
44. Hunt D, Raivich G, Anderson PN. Activating transcription factor 3 (ATF3) and the nervous system. *Front Mol Neurosci.* 2012;5(Article7):1–17. doi:10.3389/fnmol.2012.00007
45. Ikeda H, Kiritoshi T, Murase K. Contribution of microglia and astrocytes to the central sensitization, inflammatory and neuropathic pain in the juvenile rat. *Mol Pain.* 2012;8(II):1–10. doi:10.1186/1744-8069-8-43
46. Kawaguchi M, Kato H, Nakano M, Goshima S, Matsuo M. Clinical features of bone metastasis with extraosseous soft-tissue mass in prostate cancer patients. *BJR Open.* 2019;1(1):20180042.
47. Grässel S, Muschter D. Peripheral nerve fibers and their neurotransmitters in osteoarthritis pathology. *Int J Mol Sci.* 2017;18(5). doi:10.3390/ijms18050931
48. Raju G, Katiyar N, Vadukumpully S, Shankarappa SA. Penetration of gold nanoparticles across the stratum corneum layer of thick-skin. *J Dermatol Sci.* 2018;89(2):146–154. doi:10.1016/j.jdermsci.2017.11.001
49. Madhusudanan P, Reade S, Shankarappa SA. Neuroglia as targets for drug delivery systems: a review. *Nanomed Nanotechnol Biol Med.* 2017;13(2):667–679. doi:10.1016/j.nano.2016.08.013

Journal of Pain Research

Publish your work in this journal

The Journal of Pain Research is an international, peer reviewed, open access, online journal that welcomes laboratory and clinical findings in the fields of pain research and the prevention and management of pain. Original research, reviews, symposium reports, hypothesis formation and commentaries are all considered for publication. The manuscript

Submit your manuscript here: <https://www.dovepress.com/journal-of-pain-research-journal>

management system is completely online and includes a very quick and fair peer-review system, which is all easy to use. Visit <http://www.dovepress.com/testimonials.php> to read real quotes from published authors.

Dovepress